Properties of a two-dimensional D-wave superconductor from phenomenological susceptibility

St. Lenck and J. P. Carbotte
Department of Physics & Astronomy, McMaster University, Hamilton, Ontario, Canada L8S 4M1
(Received 20 April 1993; revised manuscript received 29 July 1993)

Using fast-Fourier-transform techniques, we calculated several properties of a two-dimensional D-wave superconductor directly from the phenomenological form of the magentic susceptibility suggested by Millis, Monien, and Pines. A BCS-type formalism is employed, but no assumptions are made about the exact form of the gap anisotropy. The results for the gap exhibit D-wave symmetry and go beyond the usual cosine minus cosine model. The results obtained are compared with those obtained from the simpler and much used separable model.

I. INTRODUCTION

The possibility that D-wave superconductivity exists in the copper oxide superconductors was recognized early on and remains an intriguing possibility that is the subject of considerable current activity, both theoretical and experimental.[1-19] Some aspects of the experimental evidence for and against D-wave superconductivity has been reviewed recently by Annett and Goldenfeld,[1] and some aspects of the theory have been reviewed by Monthoux and Pines.[2] On the theoretical side, early references include Bickers, Scalettar, and Scalapino[3] and others[4-6] while some recent references include Monthoux, Balatsky, and Pines,[7] Monthoux and Pines,[2] Millis,[8] Wermbter and Tewordt,[9] Lenck and Carbotte,[10] Nicol, Jiang, and Carbotte,[11] and many others.[12-17]

An important theoretical issue is the problem of obtaining large values of the critical temperature for a D-wave order parameter stabilized by exchange of antiferromagnetic spin fluctuations using realistic parameters. Early arguments[6,14] were given that even for large coupling to the antiferromagnetic spin fluctuations, only modest values of the critical temperature could be obtained because of large renormalization effects in the normal-state channel. The models assumed that the magnetic susceptibility can be written as a product of a separate function of energy and momentum and the momentum dependence taken to be separable in final and initial momenta and of a simple form consistent with D-wave symmetry. However, using a more realistic but phenomenological form for the susceptibility, which includes commensurate magnetic fluctuations with an incommensurate Fermi surface, Monthoux, Balatsky, and Pines[7,16] have obtained much larger values of T_c. Millis[8] has also given some arguments in support of large values of T_c coming from more realistic models of antiferromagnetic spin fluctuations. Similar conclusions are reached in the work of Lenck and Carbotte[10] who take a more fundamental approach. They calculate the magnetic susceptibility self-consistently from microscopics in a simple tight-binding band for a given value of Coulomb on-site repulsion U. For some values of the parameters, they can obtain values of T_c in the D-wave channel which are comparable in size to those observed in the oxides. Although they need to make a simple ansatz for the momentum dependence of their susceptibility at each step in the iteration process, their calculations lend further strong support to the possibility that high-T_c superconductivity might be stabilized by antiferromagnetic spin fluctuations.

Our primary concern in this paper will not be the calculation of the value of T_c from fundamental calculations. Instead, we will be interested in understanding the expected behavior for various superconducting properties resulting from a D-wave condensation in the CuO plane. There already exists a significant literature on the properties of D-wave superconductors and the closely related p-wave case.[20-29] Most calculations have involved a simple BCS model with a separable interaction as well as a few strong-coupling calculations along the same lines.

Little has been done specific to a tight-binding band in a plane, however. Here we start with the phenomenological susceptibility of Millis, Monien, and Pines which we use as a pairing interaction in a BCS gap equation for the anisotropic and temperature-dependent gap $\Delta(\mathbf{k},T)$ as a function of momentum in the first Brillouin zone (FBZ). No assumption is made for the form of $\Delta(\mathbf{k})$, and a fast-Fourier-transform technique yields a D-wave solution with zeros along the lines $\cos(k_x a)=\cos(k_y a)$, but not having the usual simplified $\cos(k_x a)-\cos(k_y a)$ form, with a the lattice parameter. Two possible choices are considered for the band structure, namely, nearest neighbors only and a case with next-nearest neighbors. Also, the chemical potential is varied close and away from the Van Hove singularity. Solutions are compared with each other and with the simpler separable case. Finally, results are given for the shifts in phonon energy and change in width as the superconducting state is entered. The temperature dependence of the magnetic-field penetration depth is also calculated and again comparisons with simpler models are offered.

II. MOMENTUM DEPENDENCE OF THE GAP

We start with the finite-temperature BCS equation involving the magnetic susceptibility $\chi(\mathbf{k}-\mathbf{k}')$ as the pairing interaction. The gap at any point $\mathbf{k}$ inside the first Brillouin zone (BZ) is

$$\Delta(\mathbf{k})=\sum_{\mathbf{k}'} -g^2\chi(\mathbf{k}-\mathbf{k}')\frac{\tanh[E(\mathbf{k}')/2k_BT]}{E(\mathbf{k}')}\Delta(\mathbf{k}') , \quad (1)$$

where

$$E(\mathbf{k})=\sqrt{\varepsilon(\mathbf{k})^2+\Delta(\mathbf{k})^2} , \quad (2)$$

with $\varepsilon(\mathbf{k})$ the single-particle dispersion relation. For a tight-binding band, we will take

$$\varepsilon(k)=2\bar{t}[\cos(k_xa)+\cos(k_ya) -2B\cos(k_xa)\cos(k_ya)-(2-2B-\bar{\mu})] , \quad (3)$$

where a is the lattice parameter and $\bar{\mu}$ is the normalized chemical potential with $\bar{t}$ the nearest-neighbor hopping-matrix element and $B\bar{t}$ the matrix element for next-nearest-neighbor hopping. For B equal to zero, we have the usual nearest-neighbor case with nesting at half filling which corresponds to $\bar{\mu}=2$. A value for B that may be realistic for $YBa_2Cu_3O_7$ is 0.45 in comparison with local-density-approximation (LDA) calculations.[30]

For the magnetic susceptibility, we will employ the phenomenologically determined form by Millis, Monien, and Pines (MMP), which in turn is based on NMR measurements.[17] It is (with ν_m the mth Matsubara frequency)

$$\chi(\mathbf{q},i\nu_m)=\frac{\chi(\mathbf{Q})}{1+\xi^2(\mathbf{q}-\mathbf{Q})^2-i\dfrac{(i\nu_m)}{\omega_{SF}}} \quad q_x>0, q_y>0 , \nu_m>0 \quad (4)$$

with $\mathbf{Q}=(\pi/a,\pi/a)$ and the parameters $\chi(\mathbf{Q})$, the magnetic coherence length ξ, and the spin fluctuation frequency ω_{SF} given by MMP. As we are using a BCS model with no retardation, the $\nu_m=0$ value of Eq. (4) is to enter in the BCS equation (1), namely,

$$\frac{\chi(Q)}{1+\xi^2(q-Q)^2} , \quad (5)$$

which is the kernel with largest $\mathbf{q}$ variation as compared with $\nu_m\neq 0$. Since we are not interested in making a microscopic calculation of T_c, this would require an Eliashberg formulation to be quantitative; the parameter g in (1) is adjusted to get any desired value of T_c.

We solve Eq. (1), which is completely defined, using a fast-Fourier-transform technique to get T_c and any solution below that temperature. We find that the converged solution had D-wave symmetry with lines of zeros at $\cos(k_xa)=\cos(k_ya)$, but is of a more general form than the lowest order

$$\eta_{\mathbf{k}}\equiv[\cos(k_xa)-\cos(k_ya)] \quad (6)$$

used in many models. In Fig. 1 we show our results for the gap as a function of momentum (k_x,k_y) in the first Brillouin zone for k_x and k_y ranging from $-\pi$ to π. Figure 1(a) applies in the case of the nearest-neighbor band. The critical temperature is 98.6 K with $\bar{t}=100$ meV and $\bar{\mu}=1.9$, which is near the Van Hove singularity. The maximum gap at $T=0$ was found to be 20.0 meV for a ratio $2\Delta_{max}/k_BT_c=4.71$, which is somewhat larger than the ideal value of 4.3 when a separable $\eta_{\mathbf{k}}$ model is used for the pairing interaction. This maximum happens to be at $(0,\pi)$, as it would in a separable model, but the data significantly deviate from such a simple behavior. This is made more clear in Fig. 1(b), which is applied to the same band structure, but now $\bar{\mu}=1.6$ farther away from the Van Hove singularity. The coupling strength g is adjusted so that $T_c=99.6$ K and $\Delta(k)$ exhibits two maxima on the edge of the Brillouin zone displaced from $(0,\pi)$. The maximum value of $\Delta(k)$ for $T=0$ is 27.0 meV, while the value of the gap at $(0,\pi)$ is only 23.9 meV. This gives a ratio of $2\Delta_{max}/k_BT_c=6.29$, which is much greater than the value 4.3 mentioned before. Finally, in Fig. 2, we show similar results for a different band structure. Here $B=0.45$, which is possibly appropriate to the case of YBCO. Note here that the maximum gap does not fall at $(0,\pi)$, where $2\Delta_{(0,\pi)}/k_BT_c=4.27$, but rather at some intermediate value of q_y for $q_x=0$ and $2\Delta_{max}/k_BT_c=4.50$. It is clear that the gap variation can be quite different from a simple $\eta_{\mathbf{k}}\cos(k_xa)-\cos(k_ya)$ model. It is clear then that our fast-Fourier-transform technique has produced solutions with D-wave symmetry, i.e., with zeros

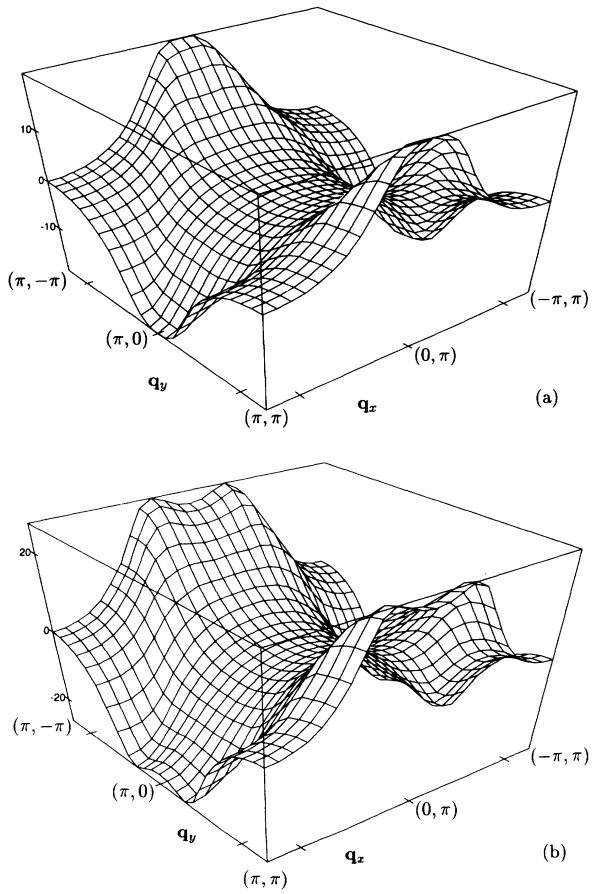

FIG. 1. Variation of the gap $\Delta(\mathbf{k})$ as a function of momentum within the Brillouin zone obtained from our fast-Fourier-transform solution of the gap equation (1). Frame (a) is for a nearest-neighbor band with $\bar{t}=100.0$ meV, $\bar{\mu}=1.9$, $T_c=98.6$ K, and $T=20.0$ K. Frame (b) is for the same band with $\bar{\mu}=1.6$, $T_c=99.6$ K, and $T=20.0$ K.

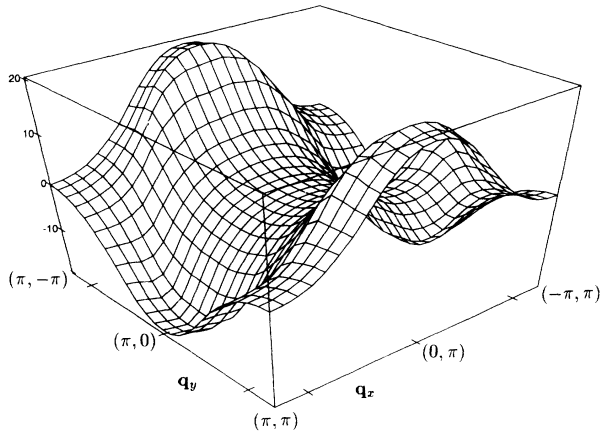

FIG. 2. Variation of the gap $\Delta(\mathbf{k})$ as a function of momentum within the first Brillouin zone obtained from our fast-Fourier-transform solution of the gap equation (1). The plot applies to a next-nearest-neighbor energy dispersion with $B=0.45$. Here $\bar{t}=100.0$ meV, $\bar{\mu}=0.6$, $T_c=105.5$ K, and $T=20.0$ K. In this case, the maximum gap ratio $2\Delta_{\max}/k_BT_c=4.51$, while $2\Delta(k=0,\pi)/k_BT_c=4.29$.

along $\cos(k_xa)=\cos(k_ya)$, but which are quite different from the simple $\eta_{\mathbf{k}}=\cos(k_xa)-\cos(k_ya)$ model.

III. PHONON SHIFTS AND WIDTHS

Certain phonon modes in the high-T_c oxides are seen in Raman-scattering studies, and the shift in frequency and change in width on entering the superconducting state can be measured. A theory for this effect has been put forward by Zeyher and Zwicknagl[31] and used by experimentalists[32,33] to extract a gap value from the pattern of behavior observed for the frequency dependence of the shift and/or the widths. The work of Zeyher and Zwicknagl[31] is based on an isotropic s-wave theory for the superconducting state and uses a strong-coupling Eliashberg formalism on the imaginary Matsubara frequency axis with a final analytic continuation of the phonon self-energy to real frequencies so as to get the physical shift and width. Marsiglio, Akis, and Carbotte[34] later improved the calculations by employing directly a real frequency axis formulation which avoids some of the numerical smearing of the results inherent in the Padé approximation used for the analytic continuation from imaginary to real axis. More recently, Nicol and Carbotte have considered the phonon self-energy in a D-wave superconductor using a simple $\eta_{\mathbf{k}}=\cos(k_xa)-\cos(k_ya)$ ansatz for the pairing potential within a BCS formalism. Here we will recalculate this quantity using the results for the momentum dependence of the gap given in the previous section.

The phonon self-energy due to the interaction with phonons is given in the lowest approximation, neglecting vertex corrections,[11,35] by

$$\pi_\lambda(\mathbf{q};i\nu_n)=T\sum_{m\mathbf{k}}|g_{\mathbf{k}+\mathbf{q},\mathbf{k}\lambda}|^2 \times\mathrm{tr}\{\tau_3G(\mathbf{k}+\mathbf{q},i\omega_m+i\nu_n)\tau_3G(,i\omega_m)\}\ , \tag{7}$$

where $G(\mathbf{k},i\omega_n)$ is the matrix Green's function in the Nambu representation and takes on the form[33]

$$G(\mathbf{k},i\omega_n)=-\frac{i\omega_n\tau_0+\varepsilon(\mathbf{k})\tau_3+\Delta(k)\tau_1}{\varepsilon(k)^2+\Delta(k)^2+\omega_n^2}\ . \tag{8}$$

In these expressions, the τ's are Pauli matrices and $i\omega_n$ ($i\nu_m$) is a fermion (boson) Matsubara frequency given by $i\pi T(2n-1)(i\pi 2m)$ with $n(m)$ integral. Also, $g_{\mathbf{k}+\mathbf{q},\mathbf{k}\lambda}$ is the electron-phonon vertex for scattering of an electron from $\mathbf{k}$ to $\mathbf{k}+\mathbf{q}$ through emission or absorption of a phonon of frequency $\omega_\lambda(\mathbf{q})$, with λ a branch index which we will suppress from this point on. Also, we are only interested in Raman scattering with $\mathbf{q}\to 0$ and will also suppress momentum dependence in (7). After some algebra assuming a BCS superconductor with gap $\Delta(\mathbf{k})$ given by our Eq. (1), the expression for the phonon self-energy shift as we go from the normal to superconducting state takes a simple form[11,34]

$$\pi(i\nu_n)=-4\sum_{\mathbf{k}}\frac{|g_{\mathbf{k},\mathbf{k}\lambda}|^2\Delta^2(\mathbf{k})}{E(\mathbf{k})[2E(k)^2+\nu_m^2]}\tanh\left[\frac{E(\mathbf{k})}{2k_BT}\right]\ . \tag{9}$$

In general, the $\mathbf{k}$ dependence of the electron-phonon coupling will affect, somewhat, the behavior of $\pi(i\nu_m)$. Since it is not known, we will take it out assuming it to be roughly constant and work with a quantity $\bar{\pi}(i\nu_m)$ in which g has been renormalized out. An analytical continuation to real frequencies $i\nu_m\to\nu+i0^+$ then gives[11,34] (for the difference with the normal state)

$$\Delta\bar{\pi}(\nu)=\sum_{\mathbf{k}}\frac{\Delta^2(\mathbf{k})}{E(\mathbf{k})^2}\left[\frac{1}{2E(\mathbf{k})+\nu+i0^+}+\frac{1}{2E(\mathbf{k})+\nu-i0^+}\right]\tanh\left[\frac{E(\mathbf{k})}{2k_BT}\right]\ . \tag{10}$$

This last expression (10) can easily be evaluated numerically from our solutions of Eq. (1) at various temperatures. In our numerical work, $i0^+$ will be taken as a finite constant related to the numerical precision of our numerical grid. For the fast Fourier transform, we use a grid of 252 points and $i0^+\simeq i(2\text{ meV})$.

Results are presented in Figs. 3(a) and 3(b) for the real and imaginary parts of $\Delta\pi(\nu+i0^+)$ as a function of frequency ν for various values of reduced temperature, namely, $T=20.0$ K (solid line), $T=40.0$ K (dotted line), $T=60.0$ K (short-dashed line), $T=80.0$ K (long-dashed line), $T=100.0$ K (next long-dashed line), and $T=110.0$ K (last long-dashed line). In this instance, $T_c=113.3$ K and the chemical potential $\bar{\mu}=0.3$, which is close to the Van Hove singularity since we are using the next-nearest-neighbor model. The first peak in the imaginary part at about 45 meV falls near twice the maximum gap value on the Fermi line. The other peak at higher energy is a reflection of the Van Hove singularities. As the temperature is increased, the gap structure, as expected, moves to lower energies as does the structure from the Van Hove singularities. These graphs are quite different

from those found previously in the work of Nicol and Carbotte. Some of the differences come from our use of second-nearest-neighbor bands, and some are due to the more complicated solution for the momentum dependence of $\Delta(k)$, which is not a simple $\eta_k=\cos(k_x a)-\cos(k_y a)$. To understand these differences a little better, we return to our simpler first-nearest-neighbor band-structure model and show results for the real and imaginary parts of $\Delta\pi(\nu)$ (solid curves) in Fig. 4. In this case, $T_c=98.6$ K and $\bar{\mu}=1.9$. The maximum gap in the FBZ is 20.0 meV, while the maximum gap on the Fermi line is 17.5 meV. Twice that value is

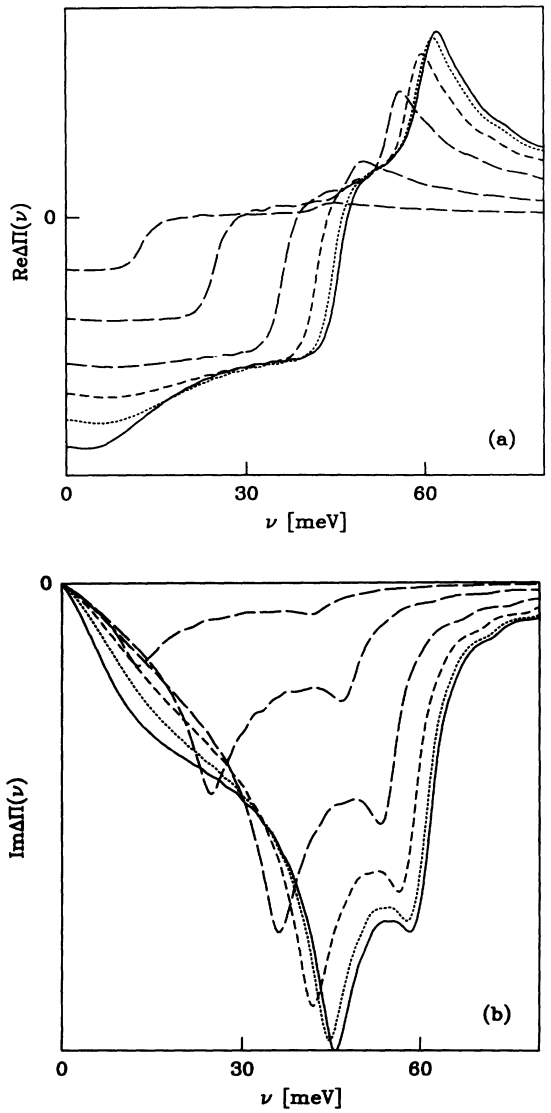

FIG. 3. Phonon self-energy $\Delta\pi(\nu)$ as a function of frequency ν for several values of temperature, namely, 20.0 K (solid line), 40.0 K (dotted line), 60.0 K (short-dashed line), 80.0 K (lower long-dashed line), 100.0 K (next long-dashed line), and 110.0 K (top long-dashed line). The calculations are for a second-nearest-neighbor band with $B=0.45$, $\bar{t}=100.0$ meV, $\bar{\mu}=0.3$ (near the Van Hove singularity), and $T_c=113.3$ K. Frame (a) is for the real part, frame (b) for the imaginary part.

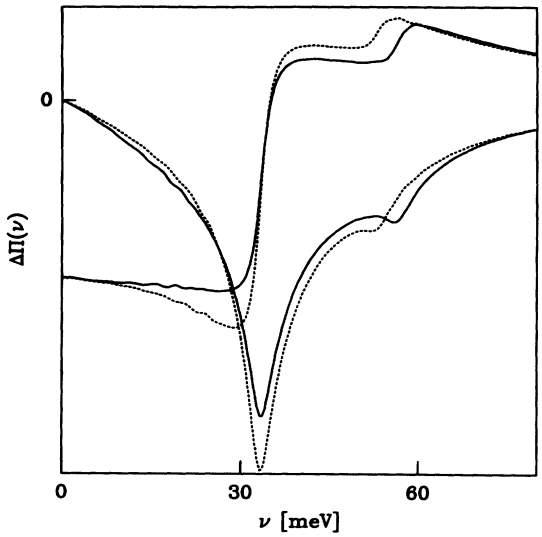

FIG. 4. Phonon self-energy $\Delta\pi(\nu)$ at $T=20.0$ K as a function of frequency ν for a nearest-neighbor band with $\bar{t}=100.0$ meV, $\bar{\mu}=1.9$ (near the Van Hove singularity), and $T_c=98.6$ K. The solid curves were obtained from our fast-Fourier-transform solutions of the gap equation (1). The dotted curves are for comparison and apply to a simple $\cos(k_x a)-\cos(k_y a)$ model with the maximum gap taken to be 17.5meV equal to the maximum value on the Fermi line obtained from our complete calculations.

the frequency at which the imaginary part of $\Delta\pi(\nu)$ shows its first minimum. Generally, the pattern of behavior in this graph is different from that of Fig. 3, reflecting the different band structure and Fermi line. In Fig. 4 the dashed lines are for a pure $\cos(k_x a)-\cos(K_y a)$ model adjusted so that the frequency of the gap structure coincides with that of the more complicated model. Even when this adjustment is made, there remain some important differences in detail among the two curves, although the qualitative nature of the variations is fully captured by the simplified model. A detailed comparison of such curves with the existing experimental data can be found in the recent work of Nicol, Jiang, and Carbotte.[35]

IV. PENETRATION DEPTH

In a bulk superconductor, an external magnetic field can only penetrate a small surface region called the penetration depth. From electrodynamics, the penetration tensor (2×2, in our case) is related to the surface impedance $Z(\omega)$ by[27,36]

$$\lambda=\lim_{\omega\to0}\frac{Z(\omega)}{i\omega u_0}\ , \tag{11}$$

with μ_0 the permeability. The surface impedance can be calculated from the electromagnetic-field response function $\mathbf{K}(\mathbf{q},\omega)$, which relates the current $\mathbf{J}(\mathbf{q},\omega)$ to the electromagnetic vector potential $\mathbf{A}(q,\omega)$ by [27,36]

$$J_i(\mathbf{q},\omega)=K_{ij}(\mathbf{q},\omega)A_j(q\omega)\ , \tag{12}$$

with i,j component indices. For specular reflection and in the London limit $q \rightarrow 0$,

$$\lambda_{ij}(T) = \left[\frac{\mu_0}{4\pi} K_{ij}(0,0) \right]^{-1/2}, \tag{13}$$

and this can be worked out in the simplest approximation to be[36,37]

$$\lambda_{ij(T)}^{-2} \sim \sum_{\mathbf{k}} \frac{\partial \varepsilon_{\mathbf{k}}}{\partial k_i} \frac{\partial \varepsilon_{\mathbf{k}}}{\partial k_j} \left[\frac{\partial f(E(\mathbf{k}))}{\partial E(\mathbf{k})} - \frac{\partial f(\varepsilon(\mathbf{k}))}{\partial \varepsilon(\mathbf{k})} \right], \tag{14}$$

where, for simplicity, we have dropped the label L for London and have left out a proportionality constant which will play no role as we will present results for the normalized quantity

$$\left[\frac{\lambda_{XX}(0)}{\lambda_{XX}(T)} \right]^2$$

as a function of reduced temperature (T/T_c). In Eq. (14), $f(x)$ is the Fermi-Dirac distribution at T. In Fig. 5 we show numerical results based on the solutions for $\Delta(\mathbf{k})$ obtained in Sec. II. The solid curve is for the nearest-neighbor model with $\bar{\mu}=1.9$, while the long-dashed curve is for the same band structure, but now $\bar{\mu}=1.6$ farther away from the Van Hove singularity. We see clearly that at low temperature both curves exhibit a linear temperature dependence, but the curve with $\bar{\mu}=1.6$ exhibits a considerably smaller slope, so that a shift in chemical potential through doping can be expected to change the overall shape of the penetration depth curve, although the linear dependence at low temperature remains. The short-dashed curve is for the next-nearest-neighbor band with chemical potential $\bar{\mu}=0.3$, while the dot-dashed curve is for the same band structure but with $\bar{\mu}=0.6$ farther away from the Van Hove singularity. It is clear that band structure affects the value of the slope of the linear law at low temperature. Also, the final dot-dashed curve is seen to have moved a considerable way toward the dotted curve, which is $1-t^2$, shown for comparison. It is perhaps of interest to note that these curves do not order according to the maximum gap to a T_c value $2\Delta^{\max}/k_B T_c$, which are 4.71, 4.85, 6.29, and 4.51, respectively, for the solid to dot-dashed curves. The situation is just more complex and shows that the temperature dependence of the London penetration depth can depend on some of the details of the underlying band structure and superconducting state. The qualitative behavior of these curves, however, is captured by the simpler separable $\cos(k_x a)-\cos(k_y a)$ model. In Fig. 5 we show the recent experimental results of Hardy *et al.*[38] which clearly show a linear variation at low temperature (open circles). It is clear, however, that their results are quite different from the present theoretical curves. As we have seen already, changes in the band structure can change the theoretical curves as can different choices of the basic interaction given by (4). To illustrate this, we show in Fig. 6 results when the antiferromagnetic coherence length is changed. The solid curve has already been presented and discussed in Fig. 5. It applies to the nearest-neighbor hopping case and is for an antiferromagnetic coherence length $\xi=2.5$. Results for two additional runs in which ξ has been halved (long-dashed

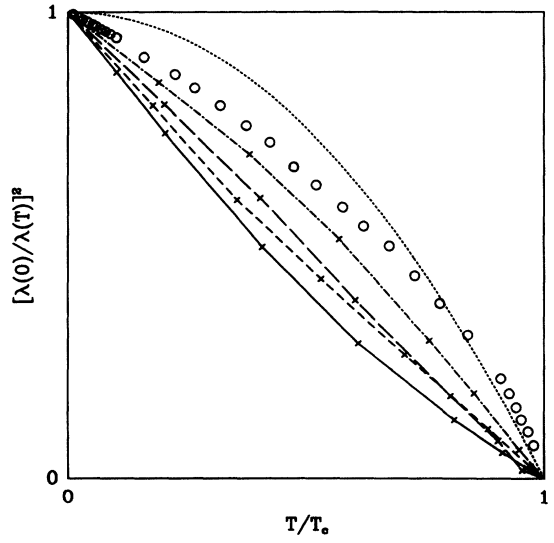

FIG. 5. Temperature (T/T_c) variation of the normalized penetration depth ratio squared $[\lambda(0)/\lambda(T)]^2$. The dotted curve is $[1-(T/T_c)^2]$ for comparison only. The solid and long-dashed curves are for the nearest-neighbor band-structure model with $\bar{\mu}=1.9$ and (near the Van Hove singularity) $\bar{\mu}=1.6$, respectively. The long-dashed and dot-dashed curves are for the next-nearest-neighbor band-structure model with $\bar{\mu}=0.3$ (near the Van Hove singularity) and $\bar{\mu}=0.6$. The open circles are data on high-quality single-crystal $YBa_2Cu_3O_7$ by Hardy *et al.* (Ref. 38).

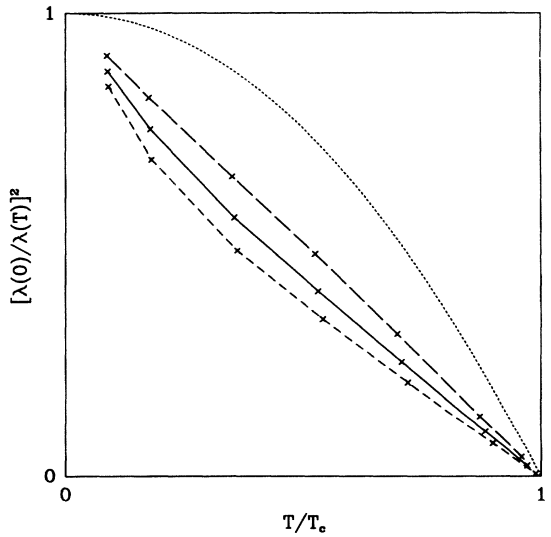

FIG. 6. Normalized square of the inverse of the penetration depth $[\lambda(0)/\lambda(T)]^2$ as a function of reduced temperature T/T_c for the nearest-neighbor band model with different values of magnetic coherence length (ξ). The solid curve is as in Fig. 5 and is for comparison. The short-dashed curve was obtained when ξ was doubled and the long-dashed curve when it was halved keeping the T_c value unchanged.

curve) and doubled (short-dashed curve) are also shown. It is clear that the temperature variation of the penetration depth is significantly affected by the choice of magnetic coherence length entering the susceptibility. Should this quantity be significantly temperature dependent, it would be strongly reflected in the penetration depth curves. It has been argued by Monthoux, Balatsky, and Pines,[7] from consideration of NMR data, that the value of ξ may be frozen in the superconducting state and so ξ may not be significantly temperature dependent.

V. CONCLUSION

In conclusion, we have calculated the detailed momentum variation of the superconducting energy gap for a BCS superconductor directly from the phenomenological magnetic susceptibility advanced by MMP on the basis of an analysis of the NMR data in the high-T_c oxide superconductors. We obtain from numerical solution of the gap equation, using a fast-Fourier-transform technique, a gap which exhibits *D*-wave symmetry, but is quite different in detail from the often used $\cos(k_x a)-\cos(k_y a)$ dependence. For values of the critical temperature appropriate to the oxides, we find that considerable differences arise as the underlying band structure is modified from a nearest-neighbor model to the next-nearest-neighbor case. Also, the position chosen for the chemical potential $\bar{\mu}$ makes a difference.

From the solutions obtained, we calculate the real and imaginary parts of the phonon self-energy difference between normal and superconducting states and find significant changes with band-structure and chemical potential values as well as some differences from previous results based on a much simpler separable $\cos(k_x a)-\cos(k_y a)$ model. When the penetration depth is considered, the temperature dependence of the reduced ratio $[\lambda(0)/\lambda(T)]^2$ is found to be linear at low temperature but with a slope that can change significantly with value of the chemical potential and band structure. The differences found for the various curves considered were not found to follow a simple pattern of classification.

ACKNOWLEDGMENTS

We would like to thank Fred Kus for his assistance with the fast Fourier transform and its implementation. This work was supported by a grant of the National Sciences and Engineering Council of Canada (NSERC) and by Canadian Institute for Advanced Research (CIAR).

[1]J. F. Annett and N. Goldenfeld, J. Low Temp. Phys. **89**, 197 (1992).
[2]P. Monthoux and D. Pines, Nuovo Cimento (to be published).
[3]N. E. Bickers, R. T. Scalettar, and D. J. Scalapino, Int. J. Mod. Phys. B **1**, 687 (1987).
[4]D. J. Scalapino, E. Loh, and J. E. Hirsch, Phys. Rev. B **34**, 8190 (1986).
[5]N. E. Bickers, S. R. White, and D. J. Scalapino, Phys. Rev. Lett. **62**, 961 (1989).
[6]A. J. Mills, S. Sachdev, and C. M. Varma, Phys. Rev. B **37**, 4975 (1988).
[7]P. Monthoux, A. V. Balatsky, and D. Pines, Phys. Rev. Lett. **67**, 3448 (1991); Phys. Rev. B **46**, 14 803 (1992).
[8]A. J. Millis, Phys. Rev. B **45**, 13 047 (1992).
[9]S. Wermbter and L. Tewordt, Phys. Rev. B **43**, 10 530 (1991).
[10]St. Lenck and J. P. Carbotte, Phys. Rev. B **46**, 14 850 (1992).
[11]E. J. Nicol, C. Jiang, and J. P. Carbotte, Phys. Rev. B **47**, 8131 (1993).
[12]H. Monien, P. Monthoux, and D. Pines, Phys. Rev. B **43**, 275 (1991).
[13]P. Monthoux and D. Pines, Phys. Rev. Lett. **69**, 961 (1992).
[14]C. M. Varma, in *High-T_c Superconductors*, edited by Harald W. Weber (Plenum, New York, 1988), p. 13.
[15]D. Pines, Physica C **185-189**, 120 (1991).
[16]P. Monthoux and D. Pines, Phys. Rev. B **47**, 6069 (1993).
[17]A. J. Millis, H. Monien, and D. Pines, Phys. Rev. B **42**, 167 (1990).
[18]S. M. Anlage and D. H. Wu, J. Supercond. **5**, 395 (1992).
[19]D. A. Bonn, P. Dosanjh, R. Liang, and W. H. Hardy, Phys. Rev. Lett. **68**, 2390 (1992).
[20]P. J. Hirschfeld, P. Wölfle, J. A. Sauls, D. Einzel, and W. O. Putikka, Phys. Rev. B **40**, 6695 (1989).
[21]W. O. Putikka, P. J. Hirschfeld, and P. Wölfle, Phys. Rev. B **41**, 7285 (1990).
[22]P. J. Hirschfeld, D. Vollhardt, and P. Wölfle, Solid State Commun. **59**, 111 (1986).
[23]H. Monien, K. Scharnberg, L. Tewordt, and D. Walker, Solid State Commun. **61**, 581 (1987).
[24]R. A. Klemm, K. Scharnberg, D. Walker, and C. J. Rieck, Z. Phys. B **72**, 139 (1988).
[25]F. Gross, B. S. Chandrasekar, D. Einzel, P. J. Hirschfeld, K. Andres, H. R. Ott, Z. Fisk, J. Smith, and J. Beuers, Z. Phys. B **64**, 175 (1986).
[26]P. J. Hirschfeld, P. Wölfle, and D. Einzel, Phys. Rev. B **37**, 83 (1988).
[27]M. Prohammer and J. P. Carbotte, Phys. Rev. B **43**, 5370 (1991).
[28]M. Prohammer and J. P. Carbotte, Phys. Rev. B **42**, 2032 (1990).
[29]A. Perez-Gonzalez and J. P. Carbotte, Phys. Rev. B **45**, 9894 (1992).
[30]T. Schneider and M. P. Sörensen, Z. Phys. B **80**, 331 (1990).
[31]R. Zeyher and G. Zwicknagl, Solid State Commun. **66**, 617 (1988); Z. Phys. B **78**, 175 (1990).
[32]B. Friedl, C. Thomsen, and M. Cardona, Phys. Rev. Lett. **65**, 915 (1990).
[33]E. Altendorf, J. Chrzanowski, and J. C. Irwin, Physica C **175**, 47 (1991).
[34]F. Marsiglio, R. Akis, and J. P. Carbotte, Phys. Rev. B **45**, 9865 (1992).
[35]E. J. Nicol, C. Jiang, and J. P. Carbotte, Phys. Chem. Solids (to be published).
[36]C. Jiang and J. P. Carbotte, Phys. Rev. B **45**, 10 670 (1992).
[37]P. Arberg, M. Mansor, and J. P. Carbotte, Solid State Commun. **86**, 671 (1993).
[38]W. N. Hardy, D. A. Bonn, D. C. Morgan, Ruixing Liang, and Kuan Zhang, Phys. Rev. Lett. **70**, 3999 (1993).